COMPARISON OF INTEGRATION METHODS FOR MULTIPATH ACOUSTIC DISCHARGE MEASUREMENTS

THOMAS TRESCH
HTA Lucerne, Switzerland, ttresch@hta.fhz.ch

PETER GRUBER
Rittmeyer Ltd, Zug, Switzerland, peter.gruber@rittmeyer.com

THOMAS STAUBLI
HTA Lucerne, Switzerland, tstaubli@hta.fhz.ch

Abstract

One of the main issues of the *acoustic discharge measurement* (ADM) is related to the accuracy of the method. The accuracy of the measurements depends on many factors such as the flow situation on site, the local geometry, care devoted to the transducer installation, the electronic devices and also the algorithms applied to evaluate discharge. The robustness of the ADM may also depend on water quality and the size of the measuring section. To estimate the overall accuracy of a measurement, individual sources of errors have to be analysed separately.

Important sources of errors arise from flow field distortions which accordingly might demand a higher number of acoustic paths to achieve the desired measuring accuracy. Further sources lie in the installation, the out-of-roundness and deformation of pipes, in cross section and eventually free surface measurement, the employed integration method and also in the protrusion effect of the acoustic transducers within the flow.

According to the appendix of the IEC 60041standard the volume flux Q in a conduit can be determined by integrating individual path readings applying a simplified *Gauss-Jacobi* integration method, where the individual path readings are weighted and added up.

One of limitations of this method described in IEC 60041 is that deviations of the integrated discharge from a true discharge value are observed even when ideal velocity distributions are calculated with theoretical equations for turbulent velocity profiles. Since velocity profiles vary as a function of Reynolds number and wall roughness, these deviations are determined by these parameters. The deviations are inherent to the method proposed in IEC 60041 as an assumed uniform velocity profile is used for individual weight calculations.

A further limitation of the method is the fixed weighting of the path velocities and thus the need for very accurate positioning of the acoustic transducers with respect to the prescribed distances d_i of the acoustic paths to the pipe centre.

To overcome these limitations Voser [1999] proposes a modified integration method with slightly modified optimum sensor positions and weighting coefficients, thus reducing the integration error by 0.1 up to 0.2 percent. Furthermore, he includes in his method the actual, measured path positions for determination of the weighting coefficients and hereby eliminates the positioning error. He names this method *OWICS* (*Optimal Weighted Integration for Circular Sections*). This new method is based on the generalized Gauss-Jacobi method, abandoning the idea of a uniform velocity distribution. Coefficients are optimized on the assumption of turbulent velocity profiles, thus adapting the method better to the physical process.

In this paper the background of the integration methods is explained in detail, and advantages of the OWICS integration method are pointed out and demonstrated for selected examples. Quantitative data showing integration uncertainty as a function of the number of paths for ideal and disturbed velocity distributions is provided.

1. Multipath Acoustic Discharge Measurement

The multipath acoustic discharge measurement (ADM) is a well established method for accurate discharge measurement, especially for large closed conduits and rectangular channels.

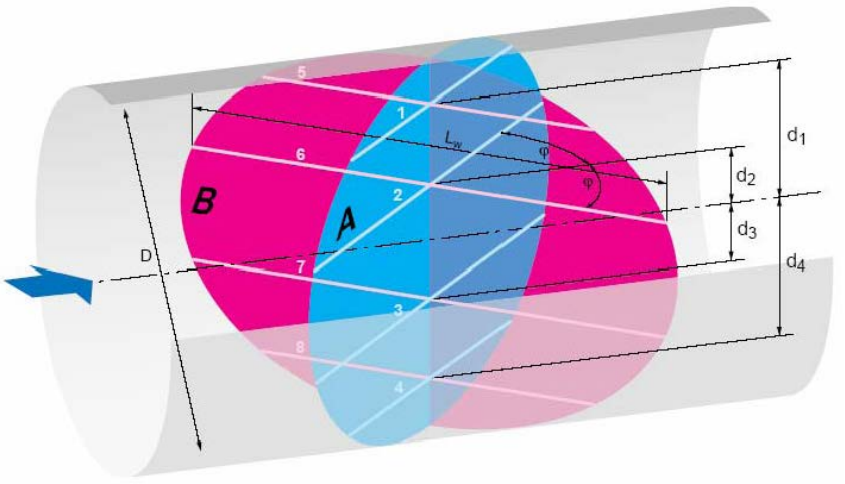

Fig. 1.1: Measurement section of an 8 path and two planes ADM

Figure 1 shows a typical 4-path, two-plane application for a closed conduit. The two planes allow compensation of cross flows effects in the measurement section. The resulting flow rate Q is given by $Q= (Q_A + Q_B)/2$.

Averaged velocities are measured on each of the acoustic paths. These path velocities are influenced by local flow disturbances and possible cross flow in the measuring section. The volume flux in the entire cross section is estimated by averaging and weighting the individual path readings. The accuracy of the method increases with larger pipe diameters and higher velocities

The following sections discuss variations in accuracy of different integration methods depending on the number of paths assumed for the cases of ideal and disturbed velocity distributions. Further focus lies on the influence of inaccuracies of sensor positions and on ways to eliminate these negative influences on volume flux determination.

2. The area flow function

The basic idea of volume flux integration is to reconstruct in a first step the velocity distribution in the flow cross section on the basis of the measured, local velocities in one acoustic plane, as e.g. the path averaged velocities $v_1,\ldots v_4$ in the arrangement of Figure 1.1

In a second step the distribution is integrated. Numerically the flow rate Q can be approximated by summing up the partial flow rates ΔQ_i for each horizontal strip, as displayed in Figure 2.1.

$$Q = \sum_{i=1}^{N} \Delta Q_i = \sum_{i=1}^{N} \bar{v}_i \cdot A_i = \sum_{i=1}^{N} \bar{v}_i \cdot l_i \cdot \Delta z \qquad (2.1)$$

The *area flow function* F(z) describes the distribution of the partial flow rates on the strips and is expressed by

$$Q = \int_{-R}^{R} F(z)dz = \lim_{N\to\infty} \sum_{i=1}^{N} \Delta Q_i \qquad (2.2)$$

Therefore, the area flow function at a given position d_i can be written as

$$F(d_i) = \bar{v}_i \cdot l_i . \qquad (2.3)$$

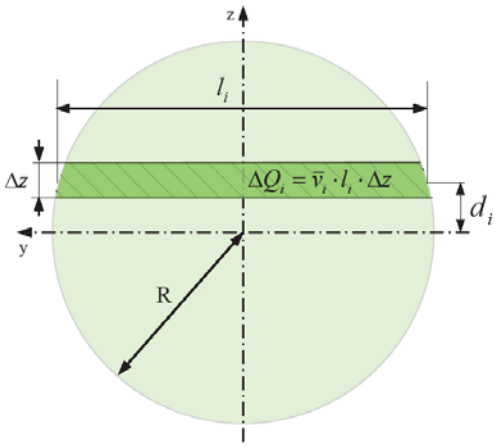

Fig. 2.1: Integration by summing up the partial flow rates

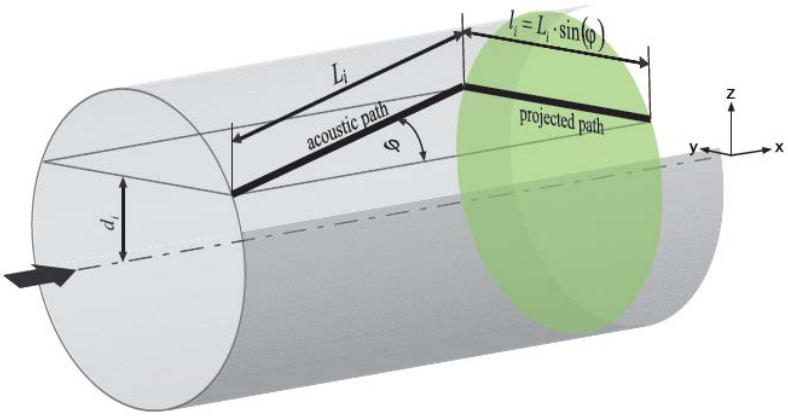

Fig.2.2: Projection of the acoustic path on the y-z-plane

The measured path velocities v_i can be projected on the y-z-plane (Fig. 2.2)

$$F(d_i) = \bar{v}_i \cdot L_i \cdot \sin(\varphi) \tag{2.4}$$

Due to the finite number of measured paths it is not possible to calculate the sum of the right hand side of the equation (2.2). For this reason the integral (2.2) is approximated by a finite sum using *weighting factors* $w_1,\ldots w_N$.

$$Q = \int_{-R}^{R} F(z)dz \cong C \cdot \sum_{i=1}^{N} w_i \cdot F(d_i) \tag{2.5}$$

where C denotes a constant. In the following section the theoretical background for determination of the weighting factors is deduced.

3. Gaussian Quadrature

3.1 General Theory

Numerical *quadrature* is the numerical calculation of the area below a curve using interpolating polynomials. This corresponds to a numerical integration to calculate a definite integral (from a to b) of a function *f(x)*

$$I = \int_a^b f(x)dx \tag{3.1}$$

The integral *I* is approximated by a finite number *N* of known values of *f(x)* at the known *abscissas* x_1, x_2, … , x_N. The *weights* $w_1, w_2,\ldots , w_N$ are chosen such that

$$I = \int_a^b f(x)dx \cong w_1 \cdot f(x_1) + w_2 \cdot f(x_2) + \ldots + w_N \cdot f(x_N) \tag{3.2}$$

Equation (3.2) is called *N-point quadrature*. For illustration the simple example of the *trapezoidal rule* is to be explained: Given are 2 values *f(0)* and *f(1)* of an unknown function *f(x)* in the interval [0,1] at the abscissas $x_1=0$ and $x_2=1$ (Figure 3.1). To approximate the integral of *f(x)* from 0 to 1 the points *f(0)* and *f(1)* are interpolated with a linear function. The area of the resulting trapezoid is calculated as

$$\int_0^1 f(x)dx \cong \frac{1}{2} f(0) + \frac{1}{2} f(1) \cdot \tag{3.3}$$

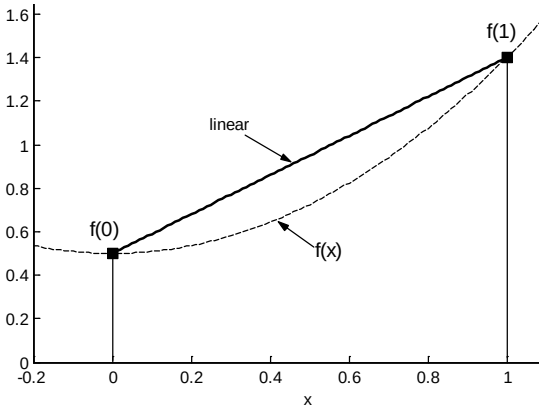

Fig. 3.1: Trapezoidal rule

According to equation (3.2) the weights are $w_1=w_2=1/2$. Except for constant or linear functions *f(x)*, the trapezoidal rule gives only an approximation of the exact integration. To minimize the error for more general

functions, better interpolations are required. For integration of quadratic functions *f(x)* numerically without error, a quadratic interpolation is required. In this case the method is called *Simpson-Rule*. Generally this class of quadrature is called *Newton-Cotes Quadrature* [Press95].

To construct Newton-Cotes formulas, firstly the abscissas are chosen to calculate the weights. By choosing the abscissas some degrees of freedom are lost. When both the abscissas and the weights are treated as unknown parameters, a much better approximation to the exact result is achieved. This method is known as *Gaussian Quadrature*. The Gaussian Quadrature enables integration of cubic polynomials with only two function evaluations (in contrast to Simpson's Rule, which is also exact for cubic polynomials but requires three function evaluations).

The (N-Point) Gaussian Quadrature provides the best numerical estimate of an integral by determining optimum abscissas $x_1, x_2, \dots, x_N$, where the function f(x) is evaluated. Therefore the method gives

- the optimal abscissas $x_1, x_2, \dots, x_N$
- and the corresponding weights $w_1, w_2, \dots, w_N$

The Gaussian Quadrature method can be extended to the numerical integration of the more general type of integrals

$$\int_a^b W(x) \cdot f(x) dx$$

where W(x) is called the *weighting function.* The commonly used weighting functions for the ADM are

Gauss-Legendre: $W(x) = 1 \qquad (-1 < x < 1)$

Gauss-Jacobi: $W(x) = (1-x)^{\alpha}(1+x)^{\beta} \qquad (-1 < x < 1)$

Other weighting functions and the corresponding abscissas and roots are listed in [Press95] or [Abra64]

The general formulation of the Gaussian Quadrature is:

Find abscissas $x_1, x_2, \dots, x_N$ and weights $w_1, w_2, \dots, w_N$ such that the integral

$$\int_a^b W(x) \cdot f(x) dx \cong w_1 \cdot f(x_1) + w_2 \cdot f(x_2) + \dots + w_N \cdot f(x_N) \qquad (3.4)$$

is exact, if *f(x)* is a polynomial of degree less then 2N.

Procedure for the Gaussian Quadrature (3.4):

COMPUTATION OF THE ABSCISSAS:

Polynomials are generated based on the recurrence

$$\begin{aligned} p_{-1} &= 0 \\ p_0 &= 1 \\ p_{j+1}(x) &= (x - a_j) \cdot p_j(x) - b_j \cdot p_{j-1}(x) \qquad (j = 0,1,\dots,N-1) \end{aligned} \qquad (3.5)$$

where

$$a_j = \frac{\int_a^b W(x) \cdot x \cdot p_j^2(x) \cdot dx}{\int_a^b W(x) \cdot p_j^2(x) \cdot dx} \qquad b_j = \frac{\int_a^b W(x) \cdot p_j^2(x) \cdot dx}{\int_a^b W(x) \cdot p_{j-1}^2(x) \cdot dx} \quad (j = 1,2,\dots,N) \qquad (3.6)$$

The abscissas $x_1, x_2, \dots, x_N$ of the N-point numerical integration (3.4) are equal to the roots (zeros) of the polynomial $p_N(x)$ generated by the recurrence (3.5).

COMPUTATION OF THE WEIGHTS

The weights are computed with the formula

$$w_j = \frac{1}{W(x_j)} \int_a^b W(x) \cdot L_j(x) \cdot dx \quad (j = 1,2,..., N) \tag{3.7}$$

where $L_j(x)$ is the j'th Lagrange Polynomial defined as

$$L_j(x) = \prod_{\substack{k=0 \\ k \neq j}}^{N} \frac{x - x_j}{x_j - x_k} \tag{3.8}$$

with the abscissas $x_1, x_2, \ldots, x_N$.

The theory of the Gaussian Quadrature is deduced in details in [Stewart96] and **[**Press95**].**

3.2 Gauss-Legendre Quadrature (IEC 41)

This example shows the application of the Gaussian Quadrature for the weighting function W(x)=1 as used for the integration in a *rectangular section* according to IEC 41.

Given are: $W(x) = 1$, $a = -1$, $b = 1$ and $N = 2$ (see equation (3.4))

To approximate the integral by

$$\int_a^b W(x) \cdot f(x) dx = \int_{-1}^{1} f(x) dx \cong w_1 \cdot f(x_1) + w_2 \cdot f(x_2)$$

the abscissas x_1, x_2 and the weights w_1, w_2 have to be determined.

According to equation (3.5) the two polynomials $p_1(x) = x$ and $p_2(x) = x^2 - \frac{1}{3}$ are needed.

The abscissas x_1 and x_2 are the roots of $p_2(x)$:

$$x_1 = \frac{1}{\sqrt{3}}, \quad x_2 = -\frac{1}{\sqrt{3}}$$

For the weights the Lagrange Polynomials are required:

$$L_1(x) = \frac{x - x_2}{x_1 - x_2}, \quad L_2(x) = \frac{x - x_1}{x_2 - x_1}$$

With (3.7)

$$w_1 = w_2 = \int_{-1}^{1} W(x) \cdot L_1(x) \cdot dx = \int_{-1}^{1} 1 \cdot L_1(x) \cdot dx = \int_{-1}^{1} \frac{x - x_2}{x_1 - x_2} \cdot dx = 1$$

The formula for the *2-point Gauss-Legendre-Quadrature* results in

$$\boxed{\int_{-1}^{1} f(x) dx \cong w_1 \cdot f(x_1) + w_2 \cdot f(x_2) = f\left(\frac{1}{\sqrt{3}}\right) + f\left(-\frac{1}{\sqrt{3}}\right)} \tag{3.9}$$

In the same way the abscissas and weights for the *3-point* and *4-point Gauss-Legendre Quadrature* are determined:

3-point:
$$\boxed{\int_{-1}^{1} f(x) dx \cong \frac{5}{9} \cdot f\left(\frac{\sqrt{15}}{5}\right) + \frac{8}{9} \cdot f(0) + \frac{5}{9} \cdot f\left(-\frac{\sqrt{15}}{5}\right)}$$

4-point: $x_1 = 0.861136$ ($w_1 = 0.347855$) ; $x_2 = 0.339981$ ($w_2 = 0.652145$)
$x_3 = -0.339981$ ($w_3 = 0.652145$) ; $x_4 = -0.861136$ ($w_4 = 0.347855$)

The first example was the 2-point-trapezoidal rule (3.3). Here, the approximation of the integration is exact only if *f(x)* is linear or constant; e.g. the degree of *f(x)* is smaller or equal to 1. With equation (3.9) the 2-point approximation on the right hand side is equal to the integral if the degree of *f(x)* is smaller or equal to 3.

In general: The N-point Gaussian-Quadrature is exact for polynomials *f(x)* with degree smaller or equal to 2N-1. (Newton-Cotes Quadrature: N-1)

3.3 Application to ADM

Rectangular sections:

For application of the procedure described in the example of section 3.2 to the integration of a rectangular section with length *B* and height *D* the area-flow-function *F(z)* has to be determined. Following the same steps as in section 2, the values of the area-flow-function at the z-positions d_i of the acoustic paths are given by

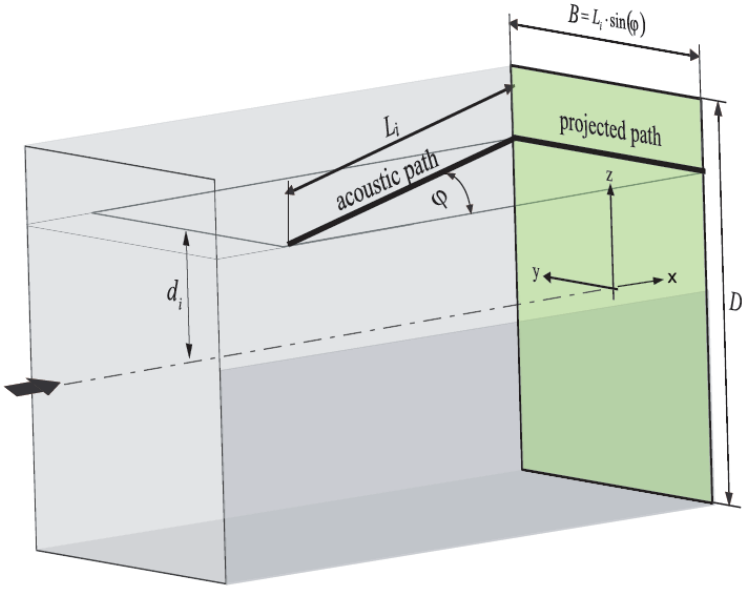

Fig. 3.2: Projection of the acoustic path to the y-z-plane in a rectangular section

$$F(d_i) = \bar{v}_i(d_i) \cdot L_i \cdot \sin(\varphi) = \bar{v}_i(d_i) \cdot B \qquad (3.10)$$

Assuming uniformly distributed velocity (v=constant) in the rectangular section, *F(z)* becomes a constant since *B* does not depend on z (see figure 3.2).

Therefore the weighting function can be chosen as W(x)=1 (*Gauss-Legendre-Quadrature*).

With the linear transformation

$$z = \frac{H}{2} \cdot x$$

the new positions determined with equation (3.9) in the case of two acoustic paths are

$$d_1 = \frac{H}{2} \cdot x_1 = \frac{H}{2\sqrt{3}},$$

$$d_2 = \frac{H}{2} \cdot x_2 = -\frac{H}{2\sqrt{3}}$$

The flow rate in the rectangular section can be approximated by

$$Q = \int_{-H/2}^{H/2} F(z)dz = \frac{H}{2}\int_{-1}^{1} F\left(\frac{H}{2} \cdot x\right)dx \cong \frac{H}{2}\left(w_1 \cdot F(d_1) + w_2 \cdot F(d_2)\right) = \frac{H}{2}\left(F(d_1) + F(d_2)\right) = \frac{B \cdot H}{2}\left(\bar{v}_1 + \bar{v}_2\right) \qquad (3.11)$$

where v_1 and v_2 are the measured (mean) velocities at the path positions d_1 and d_2. For a 4 path configuration in one acoustic plane [IEC41], the equation is

$$\boxed{Q = \frac{B \cdot H}{2} \cdot \sum_{i=1}^{4} w_i \cdot \bar{v}_i(d_i)} \qquad (3.12)$$

where the positions d_i of the acoustic paths and the weights w_i are given by

$$d_1 = -d_4 = 0{,}861136 \cdot \frac{D}{2}, \quad w_1 = w_4 = 0{,}347855$$

$$d_2 = -d_3 = 0{,}339981 \cdot \frac{D}{2}, \quad w_2 = w_3 = 0{,}652145$$

Circular sections:

For the integration in circular sections, two methods with different assumptions are introduced. The first method assumes *uniform velocity distribution* and the second one a *fully developed turbulent velocity profile*

Uniform velocity distribution: Gauss-Jacobi (IEC41) method

The integration method according to IEC41 assumes uniformly distributed flow (figure 3.3 left). The area-flow-function (see chapter 2) is given by

$$F(z) = C \cdot \left(R^2 - z^2\right)^{\kappa} \qquad (3.13)$$

with κ=0.5 and constant C .

Turbulent flow profile: OWICS [1] method

In the real flows, there is zero velocity at the wall due to friction. Figure 3.2 (right) shows a fully developed turbulent flow profile. The velocity distribution is a function of the Reynolds number *Re* and the roughness *k* of the pipe. The modified area-flow-function

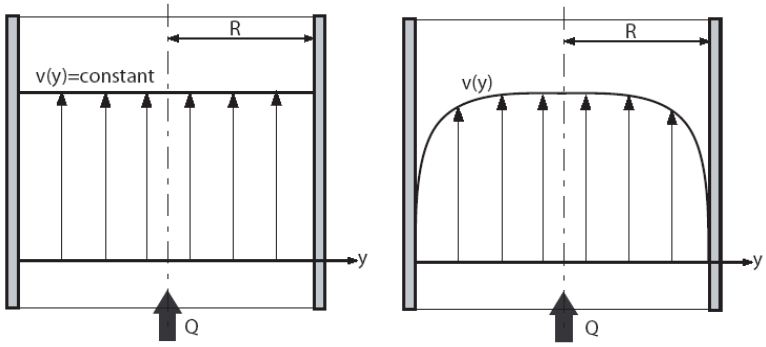

Fig. 3.3: Uniformly distributed flow (right) and a fully developed turbulent flow (left) in a circular section

$$F(z) = C \cdot \left(R^2 - z^2\right)^{\kappa} \qquad (3.14)$$

with κ=0.6 is much better adapted to the physical process (see [Voser99]) and takes zero velocities at the wall into acount.

The difference between equations (3.13) and (3.14) lies in the power κ. Both equations are based on the same theory. Since the flow rate Q is given by

$$Q = \int_{-D/2}^{D/2} F(z)dz \qquad (3.15)$$

the weighting function W(z) can be set equal to the area-flow-function F(z). In *Abramowitz* [Abra64] the Gaussian Quadrature with this weighting function W(z) is known as *Gauss-Jacobi-Quadrature* where

$$W(x) = (1-x)^{\alpha}(1+x)^{\beta} \qquad -1 < x < 1 \qquad (3.16)$$

With α=β=κ the weighting function results in

$$W(x) = \left(1-x^2\right)^{\kappa} \qquad -1 < x < 1 \qquad (3.17)$$

Equation (3.13) and (3.14) have the same structure as (3.17), as can be demonstrated by substituting x with z/R

$$F(z) = C \cdot \left(R^2 - z^2\right)^{k} = C \cdot R^{2\kappa}\left(1 - \left(\frac{z}{R}\right)^2\right)^{k} = c \cdot \left(1 - \left(\frac{z}{R}\right)^2\right)^{k} \qquad -1 < \frac{z}{R} < 1 \qquad (3.18)$$

In accordance with section 3.1, the abscissas $x_1,..,x_N$ (i.e. the path positions) for the N-point Gaussian-Quadrature with the weighting function (3.17) are the roots of the polynomial $p_N(x)$ generated with the equation (3.5).

[1] OWICS: Optimized Weighted Integration Method for Circular Sections [Voser99]

In [Press95] a simpler method for generating the polynomial $p_N(x)$ is given by the recursion formula:

$$\begin{aligned} p_{j+1} &= \frac{e_j}{c_j} x p_j - \frac{f_j}{c_j} p_{j-1} \qquad (p_{-1} \equiv 0,\ p_0 \equiv 1) \\ c_j &= (j+1)(j+2\kappa+1) \\ e_j &= (2j+2\kappa+1)(j+\kappa+1) \\ f_j &= (j+\kappa)(j+\kappa+1) \qquad j = 0,..., N-1 \end{aligned} \tag{3.19}$$

(κ=0.5 : Gauss-Jacobi (IEC 41), κ=0.6 : OWICS)

The polynomials of the Gauss-Jacobi (IEC41) method (κ=0.5) for the case of N=4 acoustic path in one acoustic plane are

$$p_1(x) = \frac{3}{2}x, \quad p_2(x) = \frac{5}{2}x^2 - \frac{5}{8}, \quad p_3(x) = \frac{35}{8}x^3 - \frac{35}{16}x, \quad p_4(x) = \frac{63}{8}x^4 - \frac{189}{32}x^2 + \frac{63}{128} \tag{3.20}$$

The roots (=abscissas) of the polynomial $p_4(x)$: $x_1 = -x_4 = 0.809017,\ x_2 = -x_3 = 0.309017$

In the same way the polynomials, the abscissas and the weights for the OWICS method (κ=0.6) are determined.

The ideal positions $d_1,..,d_4$ (fig. 3.4) and the weightings $w_1,\ldots,w_4$ (equation 3.7) of the acoustic transducers in a circular pipe with diameter D according to IEC 41 (Gauss-Jacobi) are given by

$$d_1 = -d_4 = 0.809017 \cdot \frac{D}{2} \qquad w_1 = w_4 = 0.369317$$

$$d_2 = -d_3 = 0.309017 \cdot \frac{D}{2} \qquad w_2 = w_3 = 0.597567$$

The ideal positions and weights for the OWICS method:

$$d_1 = -d_4 = 0.799639 \cdot \frac{D}{2} \qquad w_1 = w_4 = 0.371884$$

$$d_2 = -d_3 = 0.303783 \cdot \frac{D}{2} \qquad w_2 = w_3 = 0.588228$$

The flow rate Q (see equation 2.5) can be approximated by:

$$Q = \int_{-D/2}^{D/2} F(z)dz \cong \frac{D}{2} \cdot \sum_{i=1}^{N} w_i \cdot F(z_i) = \frac{D}{2} \cdot \sum_{i=1}^{N} w_i \cdot \bar{v}_i(d_i) \cdot L_i \cdot \sin(\varphi_i) \tag{3.21}$$

Equations without integral [Voser99] for the calculation of the weight exist for 4 acoustic paths with the assumption of nonnegative d_i :

$$\begin{aligned} w_1 &= \frac{g_1 D^2 (d_3 + d_4 - d_2) - g_2 d_2 d_3 d_4}{(1 - 4d_1^2/D^2)^{\kappa}(d_1 - d_2)(d_1 + d_3)(d_1 + d_4)} \\ w_2 &= \frac{g_1 D^2 (d_3 + d_4 - d_1) - g_2 d_1 d_3 d_4}{(1 - 4d_2^2/D^2)^{\kappa}(d_2 - d_1)(d_2 + d_3)(d_2 + d_4)} \\ w_3 &= \frac{g_1 D^2 (d_1 + d_2 - d_4) - g_2 d_1 d_2 d_4}{(1 - 4d_3^2/D^2)^{\kappa}(d_3 - d_4)(d_1 + d_3)(d_2 + d_3)} \\ w_4 &= \frac{g_1 D^2 (d_1 + d_2 - d_3) - g_2 d_1 d_2 d_3}{(1 - 4d_4^2/D^2)^{\kappa}(d_4 - d_3)(d_1 + d_4)(d_2 + d_4)} \end{aligned} \tag{3.22}$$

where $g_1 = 0.0900812$, $g_2 = 1.5133647$ for the OWICS method and $g_1 = 0.098175$, $g_2 = 1.570796$ for the Gauss-Jacobi (IEC41) method.

The abscissas d_i and the weights w_i for the Gauss-Jacobi and the OWICS methods for N=1,2,…,9 are listed in the following table:

	GAUSS-JACOBI (IEC 41) (κ=0.5)		**OWICS** (κ=0.6)	
Number of Paths N	Abscissas $d_i/(D/2)$	Weights w_i	Abscissas $d_i/(D/2)$	Weights w_i
1	0	1.570796	0	1.513365
2	±0.5	0.906899	±0.487950	0.890785
3	0	0.785398	0	0.768693
	±0.707106	0.555360	±0.695608	0.553707
4	±0.309017	0.597566	±0.303783	0.588228
	±0.809017	0.369317	±0.799639	0.371884
5	0	0.523598	0	0.515768
	±0.500000	0.453449	±0.493266	0.448857
	±0.866025	0.261799	±0.858534	0.265433
6	±0.222520	0.437546	±0.219676	0.432160
	±0.623489	0.350885	±0.616712	0.348913
	±0.900968	0.194726	±0.894939	0.198413
7	0	0.392699	0	0.388174
	±0.382683	0.362806	±0.3785145	0.359340
	±0.707106	0.277680	±0.7007971	0.277122
	±0.923879	0.150279	±0.9189577	0.153700
8	±0.173648	0.343762	±0.171872	0.340324
	±0.500000	0.302299	±0.495335	0.300163
	±0.766044	0.224375	±0.760343	0.224578
	±0.939692	0.119387	±0.935614	0.122463
9	0	0.314159	0	0.311216
	±0.309017	0.292783	±0.306222	0.296281
	±0.587785	0.254160	±0.583053	0.252911
	±0.809017	0.184658	±0.803925	0.185265
	±0.951057	0.097081	±0.947631	0.099815

4. Gauss-Jacobi and OWICS with examples

The turbulent velocity distribution depends on the Reynolds number *Re* and the roughness k_s of the conduit wall. The equations required to approximate the velocity profiles base on the logarithmic laws described in [Schlichting96]. The chosen parameters are:

Range of Reynolds numbers (Re)	:	$10^5 \ldots 10^8$	[-]
Roughness (k_s/D)	:	10^{-5}, 10^{-4} and 10^{-3}	[m]

4.1 Comparison Gauss-Jacobi (IEC41) / OWICS

IEC41 suggests using at least 4 paths for proper determination of the discharge. A comparison of the two methods is shown in Figure 4.1.for a 4 path ADM in one acoustic plane.

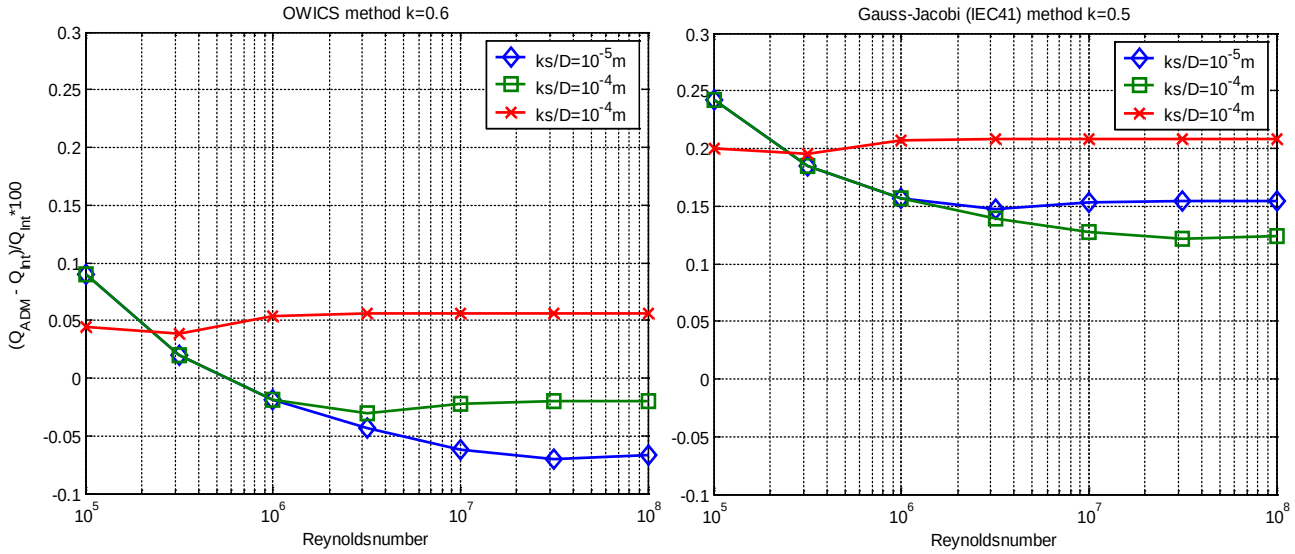

Fig. 4.1: Error of the OWICS and Gauss-Jacobi (IEC41) method for a 4 path (one acoustic plane) ADM as a function of the Reynolds number and the roughness k_s.

The average of all the integration errors (figure 4.1) yields the following results:

	OWICS	**Gauss-Jacobi (IEC41)**
Mean Error [%]	0,01	0,18

Due to the assumption of a uniform velocity profile, the method based on the Gauss-Jacobi (IEC41) method produces a systematic error. A simpler approach is to describe the turbulent velocity profile v(r) by the following approximation:

$$v(r) = v_{\max} \cdot \left(1 - \frac{r}{R}\right)^{\frac{1}{n}} \qquad (4.1)$$

where n is a function of the Reynolds number Re and the wall roughness k. The simulated integration errors on the basis of the velocity profile given with formula (4.1) are illustrated in Figure 4.2 for varying *n*.

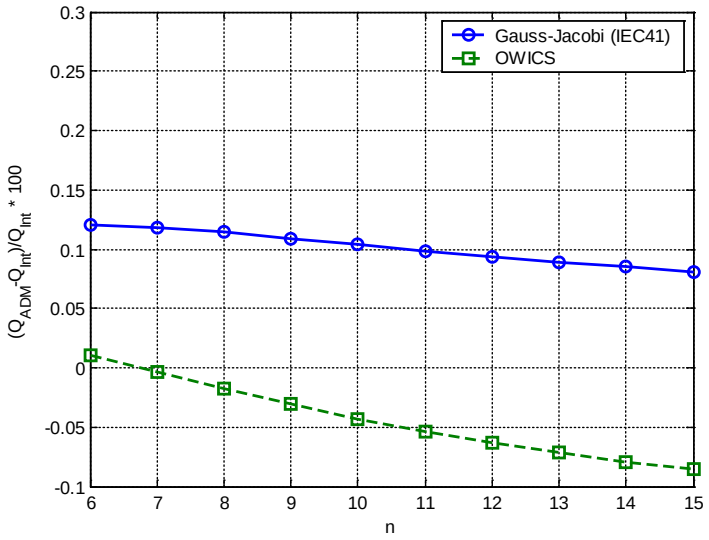

Fig. 4.2: Error of the OWICS and Gauss-Jacobi method for a 4 path (one plane) ADM as a function of n.

4.2 Influence of the number of path

According to the theory of the Gaussian quadrature, the error should decrease when increasing the number of acoustic paths. This is confirmed by simulations as shown in Figure 4.3. These simulations are based again on the approximated velocity profile of formula (4.1) with the exponent n set to 10.

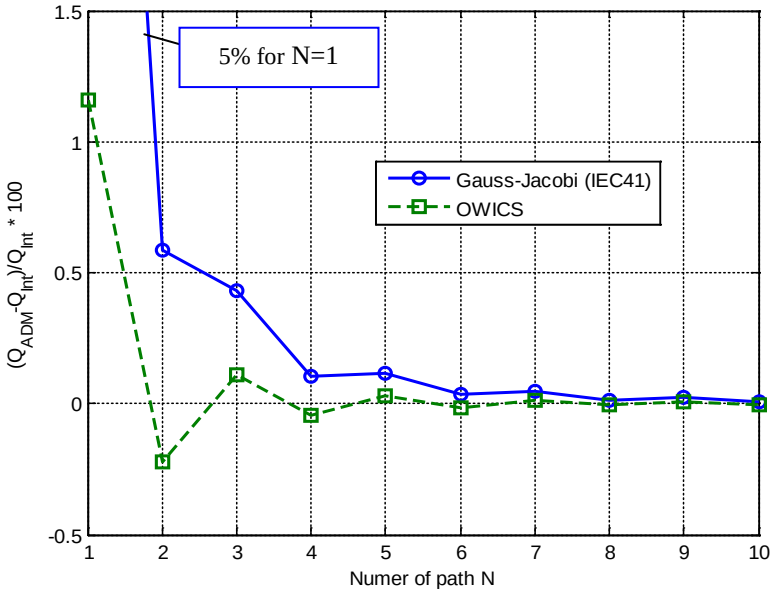

Fig. 4.3: Influence of the number of path for a 4 path (one acoustic plane) ADM

4.3 A disturbed velocity profile

In a next step the influence of a disturbed velocity profile is investigated. The disturbed profile is generated with the formula of Salami [SAL72]:

$$v(r,\varphi) = (1-r)^{\frac{1}{9}} + 3.32 \cdot r \cdot (1-r)^2 \cdot e^{-0.5\cdot\varphi} \cdot \sin(\varphi) \qquad (4.2)$$

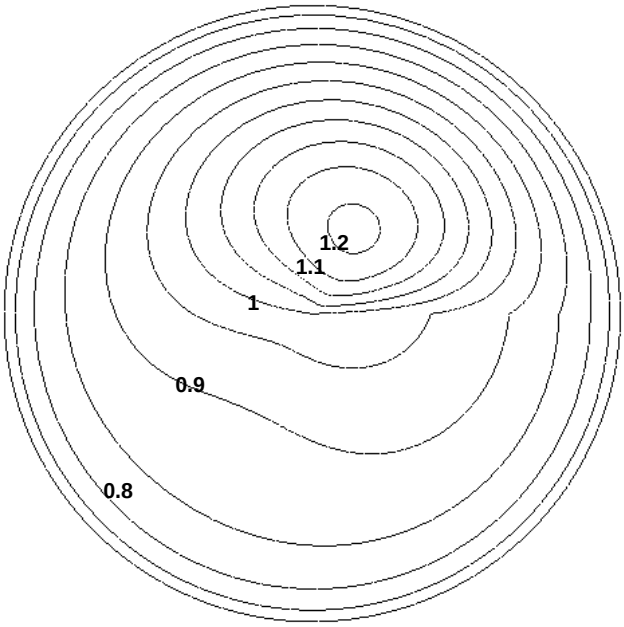

Fig. 4.4: Lines of constant velocities for the disturbed profile (4.2).

where φ denotes the angle from 0 to 2π. The radius of the circular section is set to 1. Some lines of constant velocities are illustrated in figure 4.4. In the case of an asymmetric profile, the error due to integration depends on the installation angle α of the acoustic paths.

In figure 4.5 the integration errors with the Gauss-Jacobi (IEC41) method and the OWICS method for a 4- path (in one plane) ADM for different angels α are plotted.

For both methods, the angle α = 0° yields maximum error.

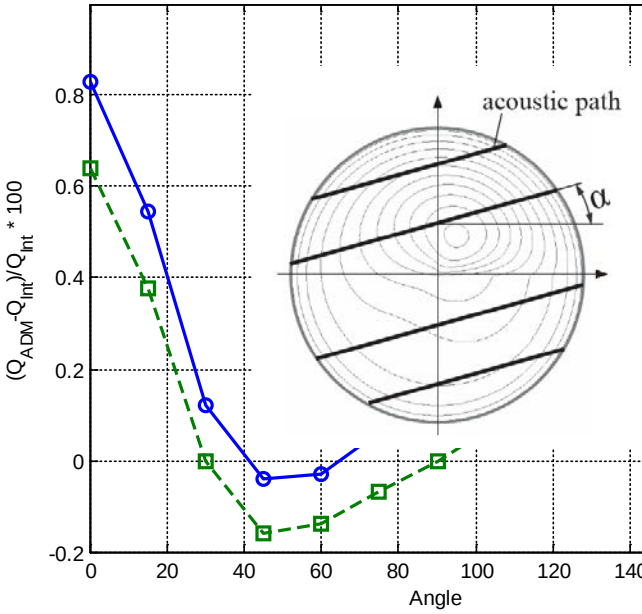

Fig. 4.5: Integration error for different installation angles α for 4 acoustic paths in one plane.

By increasing the number of paths N in one acoustic plane in the case of α=0°, the error is reduced, as illustrated in figure 4.6.

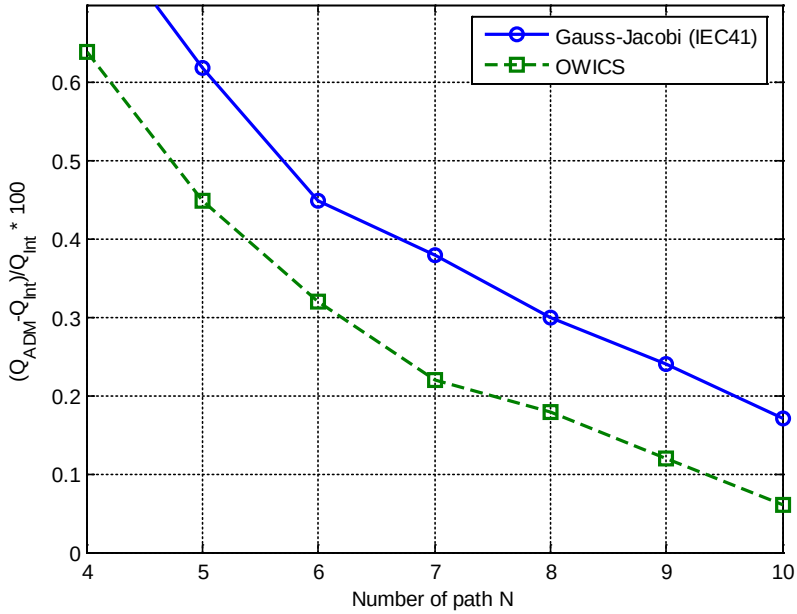

Fig. 4.6: Influence of the number of paths in case of a heavily disturbed profile (angle α=0)

4.4 Influence of non-ideal path positions

Below it is assumed that one of the acoustic paths, inner or outer, is malpositioned. If the altered weights of the new position is not taken into account, then the Gauss-Jacobi (IEC41) method shows errors increasing linearly in proportion to the degree of malpositioning (Figures 4.7 and 4.8).

If the weights of altered positions are corrected for the Gauss-Jacobi (IEC41) and the OWICS methods, the error becomes smaller (modified Gauss Jacobi), and even almost zero for the OWICS method.

Inner Path:

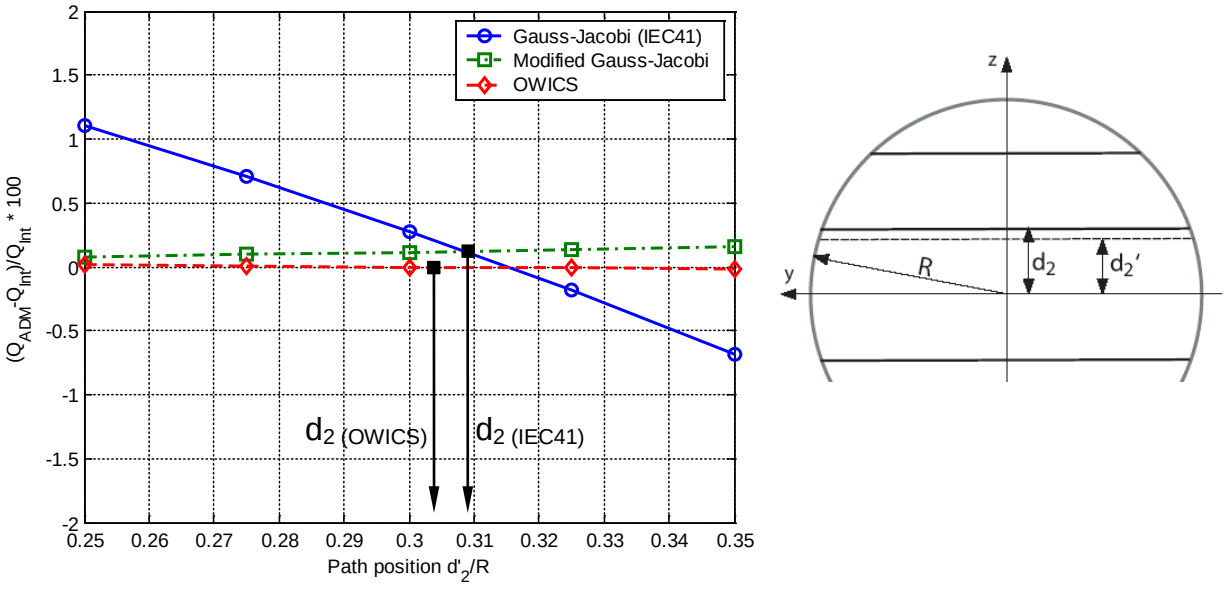

Fig. 4.7: Influence of the path position of an inner path

Outer Path:

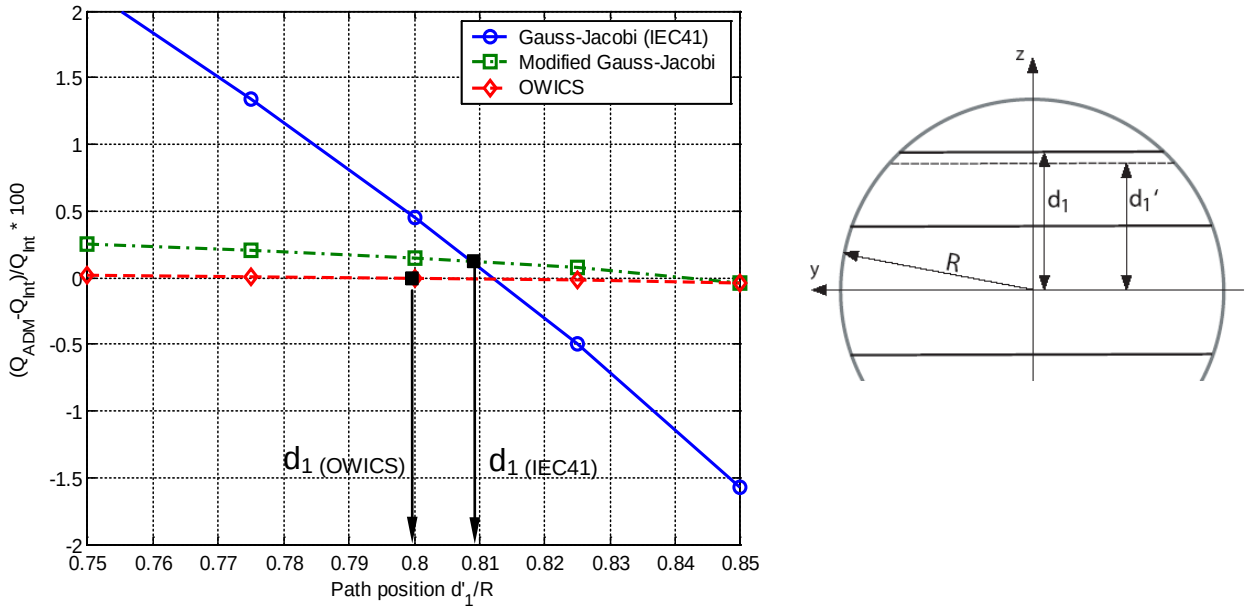

Fig. 4.8: Influence of the path position of an outer path

5. Conclusion

In comparison to the Gauss-Jacobi (IEC41) method, the OWICS method shows the following advantages:

Installation	Less sensitive to malpositioning (position must be measured and weights are calculated using the actual path positions)
Change of the integration method	ADM installed on the basis of IEC41 can easily be adapted to the OWICS by slightly modifying the weights used for integration of the volume flux.
Implementation	Basic concepts of integration remain the same. Mathematically OWICS is also based on the Gauss Jacobi Quadrature method. Only one constant has to be modified.
Process	Physically correct boundary conditions are used. The assumption of a turbulent profile with zero velocities is better adapted to the physical process.

α

e to the considerable increase of accuracy and insensitivity of the OWICS integration method to flow profile variation and to positioning of the transducers, the classical method described in IEC41 should be refined and supplemented with the elements of the OWICS method.

References

Abra64

M. Abramowitz and I. A. Stegun: Handbook of mathematical functions, (Available at: http://www.math.sfu.ca/~cbm/aands/toc.htm)

IEC41

CEI/IEC 60041: *Field acceptance tests to determine the hydraulic performance of hydraulic turbines, Storage, pumps and pump turbines*, IEC 1991

Press95

W.H. Press, S.A. Teukolsky, W.T. Vetterling, and B.P. Flannery, *Numerical Recipes in C, Second edition*, Cambridge University Press, 1995. (The same book exists for the Fortran language). (Available at http://cfata2.harvard.edu/nr/)

Sal72

L.A. Salami: *Errors in the velocity-area method of measuring asymmetric flows in circular pipes*, Modern Developments in Flow Measurement 1972.

Stewart96

G.W. Stewart: *Afternotes on Numerical Analysis*, SIAM 1996

Schlichting96

H. Schlichting, K. Gersten: *Grenzschichttheorie, 9.*, Springer 1996

Voser99

A.Voser: A*nalyse und Fehleroptimierung der mehrpfadigen akustischen Durchflussmessung in Wasserkraftanlagen*, ETH Zürich Dissertation Nr. 13102, 1999